Neurobiology of Disease 43 (2011) 598–608

Contents lists available at ScienceDirect

Neurobiology of Disease

journal homepage: www.elsevier.com/locate/ynbdi

Systemic delivery of NEMO binding domain/IKKγ inhibitory peptide to young *mdx* mice improves dystrophic skeletal muscle histopathology

Daniel P. Reay [b,1], Michele Yang [b,g,1], Jon F. Watchko [d], Molly Daood [d], Terrence L. O'Day [e], Khaleel K. Rehman [c], Denis C. Guttridge [f], Paul D. Robbins [c], Paula R. Clemens [a,b,c,*]

[a] *Neurology Service, Department of Veterans Affairs Medical Center, Pittsburgh, PA 15240, USA*
[b] *Department of Neurology, University of Pittsburgh, Pittsburgh, PA 15213, USA*
[c] *Department of Microbiology and Molecular Genetics, University of Pittsburgh, Pittsburgh, PA 15213, USA*
[d] *Department of Pediatrics, Magee-Women's Research Institute, University of Pittsburgh, Pittsburgh, PA 15213, USA*
[e] *MedImmune, Inc., Gaithersburg, MD 20878, USA*
[f] *Department of Molecular Virology, Immunology and Medical Genetics, The Ohio State University, Columbus, OH 43210, USA*
[g] *Department of Pediatrics, Section of Neurology, University of Colorado Denver, Aurora, CO 80045, USA*

ARTICLE INFO

Article history:
Received 5 January 2011
Revised 1 April 2011
Accepted 14 May 2011
Available online 23 May 2011

Keywords:
Duchenne muscular dystrophy
mdx mouse
Histopathology
Muscle necrosis
Muscle regeneration
Specific force
Lengthening activation
Protein transduction domain
NEMO binding domain peptide
NF-κB

ABSTRACT

The activation of nuclear factor κB (NF-κB) contributes to muscle degeneration that results from dystrophin deficiency in human Duchenne muscular dystrophy (DMD) and in the *mdx* mouse. In dystrophic muscle, NF-κB participates in inflammation and failure of muscle regeneration. Peptides containing the NF-κB Essential Modulator (NEMO) binding domain (NBD) disrupt the IκB kinase complex, thus blocking NF-κB activation. The NBD peptide, which is linked to a protein transduction domain to achieve *in vivo* peptide delivery to muscle tissue, was systemically delivered to *mdx* mice for 4 or 7 weeks to study NF-κB activation, histological changes in hind limb and diaphragm muscle and *ex vivo* function of diaphragm muscle. Decreased NF-κB activation, decreased necrosis and increased regeneration were observed in hind limb and diaphragm muscle in *mdx* mice treated systemically with NBD peptide, as compared to control *mdx* mice. NBD peptide treatment resulted in improved generation of specific force and greater resistance to lengthening activations in diaphragm muscle *ex vivo*. Together these data support the potential of NBD peptides for the treatment of DMD by modulating dystrophic pathways in muscle that are downstream of dystrophin deficiency.

Published by Elsevier Inc.

Introduction

Dystrophin deficiency causes muscle degeneration in Duchenne muscular dystrophy (DMD) patients and in the *mdx* mouse, a murine model for DMD (Bulfield et al., 1984). Dystrophin, a 427 kDa cytoskeletal protein expressed from the X-linked dystrophin gene, provides structural stability and functional signaling from the internal cytoskeleton to the extracellular matrix through the dystrophin–glycoprotein complex, (DGC) (Ervasti et al., 1990; Ervasti and Campbell, 1991; Zubrzycka-Gaarn et al., 1988). Disruption of the DGC, due to absence or truncation of dystrophin protein, causes the dystrophic phenotype of progressive muscle necrosis, inflammation, and fibrosis. Critical intracellular pathways that mediate the inflammatory responses to muscle sarcolemmal damage and attempted regeneration are central to the pathogenesis of dystrophic changes in muscle. By these mechanisms, the detrimental structural defects of dystrophin deficiency are compounded (Guttridge, 2004). The only treatments currently available for DMD can, at best, delay progression of the disease.

Nuclear factor κB (NF-κB) is a transcription factor that is crucial for development, cell survival and innate immunity, and can regulate genes encoding a wide range of targets from growth factors to cytokines (Verma, 2004). The 5 family members of the NF-κB family are p50, p52, RelA/p65, c-Rel and RelB, and they exist as homo- or heterodimers. When bound to the inhibitor protein IκB in the cytoplasm of mammalian cells, NF-κB remains in an inactive state. However, upon induction by specific cell stimuli, such as TNF-α or IL-1β, the IκB kinase (IKK) complex phosphorylates the IκB inhibitory protein (IκB). Once phosphorylated, IκB is targeted for ubiquitin-mediated proteosomal degradation, exposing the NF-κB subunits' nuclear localization signal, leading to nuclear translocation whereby the NF-κB dimers regulate transcription (Häcker and Karin, 2006).

* Corresponding author at: S520 Biomedical Science Tower, University of Pittsburgh, Department of Neurology, Pittsburgh, PA 15213, USA. Fax: +1 412 648 8081.
E-mail address: pclemens@pitt.edu (P.R. Clemens).
[1] Shared first authorship.
Available online on ScienceDirect (www.sciencedirect.com).

0969-9961/$ – see front matter. Published by Elsevier Inc.
doi:10.1016/j.nbd.2011.05.008

Increased levels of NF-κB activation are observed in muscle of DMD patients and the *mdx* mouse. A heterozygous deletion of the p65 subunit of NF-κB on the *mdx* genetic background (*mdx*;p65$^{+/-}$) resulted in improved muscle histopathology characterized by decreased necrosis and increased regeneration, supporting the crucial role that the NF-κB p65 subunit plays in muscle health and points to a potential target for DMD therapy (Acharyya et al., 2007). Treatment of *mdx* mice *in vivo* with therapies targeted to interrupt NF-κB activation have been previously reported to improve the dystrophic phenotype, including infliximab (Grounds and Torrisi, 2004), N-acetylcysteine (NAC) (Whitehead et al., 2008), and pyrrolidine dithiocarbamate (PDTC) (Messina et al., 2004).

Peptide-based approaches to interrupt NF-κB activation have been developed to test for therapeutic efficacy in disease models. The NF-κB Essential Modulator (NEMO) binding domain (NBD) peptide utilized in this study shares sequence homology with the IKKβ subunit of the IKK complex. NBD peptide prevents formation of the IKK complex and thereby decreases the activation of NF-κB (May et al., 2000). The NBD peptide is synthesized as a fusion peptide with a protein transduction domain (PTD) to facilitate intra-cellular delivery (Strickland and Ghosh, 2006).

PTDs are small, naturally occurring or synthetic peptides with the robust ability to cross cell membranes and transport larger molecules into cells. PTDs can be either cationic or hydrophobic and may be tissue-specific (Tilstra et al., 2007). Cationic PTDs, such as the HIV-transactivator of transcription (TAT) or 8 lysines (8K), bind heparin on the cell surface (Hakansson et al., 2001; Rusnati et al., 1997). Another naturally occurring cationic PTD, *Drosophila* Antennapedia (Antp), also binds to cell surface glycosaminoglycans (Tilstra et al., 2007). After cell surface binding, the PTD and fused cargo are internalized by macropinocytosis and released into the cytoplasm (Noguchi and Matsumoto, 2006).

Prior biodistribution studies have been performed with PTD-delivered peptides. The uptake of streptavidin-Cy3-linked PTD into cells has been shown previously in cultured cells (Dave et al., 2007; Mi et al., 2000). One *in vivo* study showed uptake of streptavidin-Cy3-linked PTD into spleen and mesenteric lymph nodes within 30 min of intraperitoneal administration (Dave et al., 2007). To complement PTD-peptide uptake studies with functional uptake studies, Khaya and Robbins (Khaja and Robbins, 2010) linked different PTDs to the NEMO binding domain peptide (NBD) and performed studies of PTD delivery of the functional NBD cargo. Schwarze et al. showed uptake of a TAT-FITC peptide in skeletal muscle after intraperitoneal administration to mice (Schwarze et al., 1999).

In this study, we explore the ability of NBD, fused to different cationic PTDs, to inhibit activation of NF-κB in muscle of the *mdx* murine model for DMD, to ameliorate the pathology of skeletal muscle in both hind limb and diaphragm in treated *mdx* mice and to improve physiological functioning of diaphragm muscle, tested by analysis of *ex vivo* force production and resistance to lengthening activations.

Materials and methods

Synthesis of fusion peptides

Fusion peptides of wild-type or mutant NBD sequence with PTD sequence (different PTD sequences are described below) were synthesized at the Peptide Synthesis Facility (University of Pittsburgh, Pittsburgh, PA). The PTDs utilized in this study are the naturally occurring TAT-NBD (amino acid sequence: GYGRKKRRQRR), the Antp-NBD (amino acid sequence: RQIKIWFQNRRMKWKK) and 8K-NBD (amino acid sequence: KKKKKKKK). PTDs were linked to either an 11-amino acid wild-type NBD peptide, representing the binding site of IKKβ subunit, (amino acid sequence: TALDWSWLQTE) or mutant NBD peptide in which the tryptophan residues were replaced with alanine residues (amino acid sequence: TALDASALQTE). Fusion peptides contained an N-terminal PTD linked to a C-terminal NBD wild-type or mutant peptide by a 2 glycine spacer (GG).

Mice and administration of fusion peptides

C57BL/10/J and C57BL/10ScSn-*Dmd*^{mdx}/J (*mdx*) mice were purchased from The Jackson Laboratory (Bar Harbor, ME) and were housed at the University of Pittsburgh, Biomedical Science Tower South Animal Housing Facility in specific pathogen-free, controlled light and humidity environmental conditions and received unrestricted access to food and water. Mice were sacrificed by carbon dioxide inhalation, followed by cervical dislocation to ensure death, prior to muscle harvesting. Studies were approved by the University of Pittsburgh Institutional Animal Care and Use Committee.

Control EMSA analysis was performed on untreated C57BL/10J and *mdx* mice at 4.5, 9, and 12 weeks of age. For EMSA studies on muscle from PTD-NBD peptide treated *mdx* mice, muscle was collected from 8K- and TAT-NBD and saline treated 9 week old mice after a single intraperitoneal injection of 10 mg/kg peptide or saline. For EMSA studies on muscle from Antp-NBD treated *mdx* mice, muscle was collected after treatment with 200 μg peptide, 3 times per week for 4 weeks (n = 3 per group).

In the 4 week experimental peptide study, sex-matched groups of 4.5 week old *mdx* mice were each administered intraperitoneal injections of PTD-NBD peptide dosed at 10 mg/kg 3 times per week (every other day) for 4 weeks (n = 8). For the 7 week experimental peptide study, sex-matched, 4 week old *mdx* mice were each administered intraperitoneal injections of PTD-NBD peptide dosed at 10 mg/kg or saline diluent alone 3 times per week for 7 weeks (n = 8). At the time of sacrifice, diaphragm muscle from experimental and control animals in the 7 week study was analyzed *ex vivo* for force production and resistance to lengthening activations as described below.

Ex vivo force analysis of costal diaphragm

To perform the *ex vivo* functional analysis, experimental and control mice were anesthetized with 50 mg/kg pentobarbital followed by costal diaphragm excision with the rib origin and central tendon insertion intact. Diaphragm specific force (peak isometric tetanic force normalized for muscle cross-sectional area) and isometric force generation during repetitive isovelocity lengthening activations were performed as previously described (Watchko et al., 2002, 1994).

Immunohistochemical analysis of treated and control mice

For 4 week peptide treatment studies, tibialis anterior and whole diaphragm muscles were harvested and snap frozen in dry ice-cooled isopentane from mice sacrificed 24 h after final fusion peptide injection (treated) or from age-matched *mdx* and C57BL/10 untreated control animals. Tissues were sectioned at 10 μm and analyzed for necrosis by labeling with a fluorescein-labeled horse anti-mouse (H + L) IgG antibody (1:200) (Vector Laboratories, Burlingame, CA). Tissue sections were analyzed for regeneration by immunohistological detection of embryonic myosin heavy chain (eMyHC) expression. For immunohistology detecting eMyHC, endogenous biotin was blocked with the Biotin–Avidin Blocking Kit and mouse IgG was blocked using the Vector M.O.M. Kit (Vector Laboratories, Burlingame, CA) followed by incubation with eMyHC supernatant antibody (1:10), biotinylated goat anti-mouse IgG secondary and streptavidin Alexa 488 (1:1500) (Invitrogen, Carlsbad, CA) tertiary antibodies. The eMyHC monoclonal antibody, F1.652, developed by Helen Blau, was obtained from the Developmental Studies Hybridoma Bank developed under the auspices of the NICHD and maintained by the University of Iowa, Department of Biological Sciences, Iowa City, IA 52242. All sections were co-immunostained with rabbit anti-collagen IV (Millipore Corporation, Billerica, MA) primary

and fluorescein-goat anti-rabbit (Sigma-Aldrich, St. Louis, MO) secondary antibodies to visualize muscle fiber membranes to facilitate total fiber counts. For quantitative analysis, 2 independent sections from separate regions of the mid-section of the muscle were counted to determine the percentage of necrotic and regenerating fibers per cross section.

For analysis of 7 week PTD-NBD peptide-treated and control, sham-treated mice, tibialis anterior muscles were harvested and snap frozen as described above. Two 10 μm sections of tibialis anterior were collected from the midsection of the muscle ~500 μm apart with approximately 1000 fibers per section for quantitative analysis. After harvesting the costal diaphragm, the muscle was divided into 1 cm lengths that were plunged into dry ice-cooled isopentane, as described above. Frozen diaphragm segments were sectioned to yield tissue cross-sections with approximately 1000 fibers per section. Two sections from each diaphragm muscle were analyzed for IgG labeling and eMyHC expression, performed as described above for 4 week peptide treatment studies.

Sections of tibialis anterior and diaphragm from mice in all treatment and control groups at both time points were also stained with hematoxylin and eosin.

Electrophoretic mobility shift assay (EMSA)

Cytoplasmic and nuclear cellular fractions were extracted from tissue samples from collected tibialis anterior and diaphragm muscles using the NE-PER Cytoplasmic and Nuclear Extraction Reagent Kit (ThermoFisher Scientific, Rockford, IL). NF-κB activity was measured by pre-incubating 5 μL of muscle nuclear extract (30 μg) with 5× Gel Shift Binding Buffer (Promega) and nuclease-free distilled water in a 9 μL final volume, followed by incubation with an α-^{32}P-deoxycytodine triphosphate labeled double-stranded DNA probe containing the NF-κB binding domain to detect NF-κB activity (Perkin Elmer, Waltham, MA). Probes were added at a count per minute (cpm) of ~100,000 in 1 μL, followed by separation on a 6% non-denaturing polyacrylamide gel. The NF-κB probe was designed previously (Guttridge et al., 1999). Briefly, 15 bp annealing oligonucleotides were annealed to 31 bp template oligonucleotides at the 3′ end of the template strand and the overhang was filled in with dNTPs in conjunction with ^{32}P dCTP using DNA Polymerase I, Large (Klenow) Fragment (Invitrogen, Carlsbad, CA) with incorporation of ~7 radioactive dCTPs per DNA molecule. Labeling reactions were purified using illustra MicroSpin G50 columns (GE Healthcare, Piscataway, NJ). Oligonucleotide sequences are as follows, with the DNA binding sequence underlined: NF-κB template: 5′-cagggctggggattccc-catctccacagtttcacttc-3′; NF-κB annealing: 5′-gaagtgaaactgtgg-3′ (Integrated DNA Technologies, Inc., Coralville, IA).

Statistics

For the 4 week peptide treatment and control data, Dunnett's test was used for pair wise comparisons with the untreated, age-matched *mdx* group as the control. In the event that normal assumptions were violated, the Wilcoxon Rank Sum test was used for pair wise comparisons. For the 7 week peptide treatment, control and densitometry data, a log10 transformation was applied prior to statistical analysis. Unless otherwise stated, Scheffe's test was used for pair-wise comparisons. In the event that the normality and homogeneity of variance assumptions were violated, and transformation did not correct the assumption violations, the Wilcoxon Rank Sum test was used for pair-wise comparisons. The MIXED procedure in SAS with repeated measures was used to model % baseline (response) for lengthening activations. A contrast statement in the MIXED procedure was utilized to make regression inference (differences in slopes) with respect to treatment groups. SAS version 9.1 was used for the statistical analyses of the data.

Results

NF-κB activity in mouse muscle nuclear extracts

EMSA analysis of NF-κB nuclear translocation in C57BL/10 and *mdx* mice at 4.5, 9, and 12 weeks of age was performed to determine levels of activity at different time points relevant to this study. As shown in Fig. 1A, C57BL/10 mice exhibit a basal level of NF-κB activation as part of development, but over time, there is a decrease in NF-κB activation in both hind limb skeletal muscle and diaphragm. In *mdx* mice, we observed high levels of NF-κB activation throughout the time frame studied in both hind limb skeletal muscle and diaphragm.

To demonstrate that the PTD-NBD peptides suppress activation of NF-κB in muscle *in vivo*, muscle tissue was collected from 9 week old *mdx* mice treated with a single 10 mg/kg intraperitoneal injection of either 8K- or TAT-NBD peptide. We also collected tissue from Antp-NBD peptide treated *mdx* mice that had received 200 μg peptide by intraperitoneal injection 3 times per week for 4 weeks, beginning at 4–5 weeks of age. Administration of each of the PTD-NBD peptides to *mdx* mice resulted in a reduction in NF-κB activation compared to saline *mdx* controls (Figs. 1B and C). The larger reduction in NF-κB activation observed in muscle from Antp-NBD peptide treated *mdx*

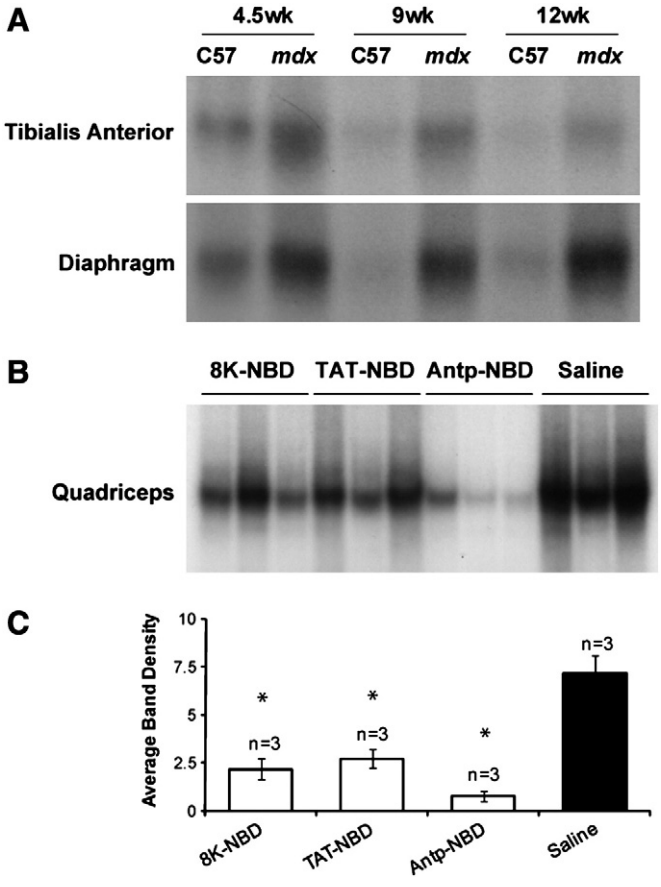

Fig. 1. EMSA analysis of NF-κB activation of control and PTD-NBD peptide treated *mdx* mice. (A) Nuclear extracts from tibialis anterior and diaphragm muscle tissue were assessed for NF-κB activation by electrophoretic mobility shift assay (EMSA) in untreated C57BL/10 and *mdx* mice at 4.5, 9, and 12 weeks of age. (B) Nuclear extracts from quadriceps muscles of 8–9-week-old 8K-, TAT- and Antp-NBD peptide treated *mdx* mice (n = 3) and saline treated *mdx* mice (n = 3) were assessed for NF-κB activation by EMSA. (C) Densitometric analysis of the blots shown in B represented as mean ± standard error. 8K- and TAT-NBD peptide treated *mdx* mice received a single injection of 10 mg/kg peptide. Antp-NBD peptide treated *mdx* mice received intraperitoneal injections of 200 μg peptide 3 times per week for 4 weeks, beginning at 4–5 weeks of age. *Indicates that the PTD-NBD peptide treatment group is significantly different from saline *mdx* control animals ($p < 0.05$). n = number of animals analyzed.

mice may reflect the sustained administration over 4 weeks as compared to a single administration with either 8K- or TAT-NBD peptide.

Analysis of tibialis anterior muscle after 4 weeks of PTD-NBD treatment

Systemic treatment of 4.5-week-old *mdx* mice with the 3 different wild-type PTD-NBD fusion peptides for a period of 4 weeks demonstrated improvement in dystrophic muscle histopathology when compared to age-matched *mdx* controls and mutant PTD-NBD peptide treated animals. Wild-type PTD-NBD treated *mdx* mice showed decreased necrosis in the hind limb tibialis anterior muscle after examination of hematoxylin and eosin stained and mouse IgG labeled sections (Fig. 2). Untreated age-matched *mdx* mice had an average of 13.6% ± 0.9% necrotic fibers per section (Fig. 3A). Treatment of *mdx* mice with TAT-NBD, 8K-NBD, and Antp-NBD fusion peptides led to decreases of 56.1%, 49.1% and 60.0%, respectively, compared to age-matched *mdx* control animals. Statistical significance was reached in the TAT-NBD and Antp-NBD treated groups ($p = 0.0091$ and $p = 0.0121$, respectively). Mutant peptide treatment did not result in significant changes in the levels of necrosis.

Furthermore, wild-type PTD-NBD peptide treated *mdx* mice displayed increased numbers of regenerating fibers in hind limb skeletal muscles in response to the different PTD-NBD fusion peptides (Figs. 2 and 3B). Immunostaining for eMyHC to identify regenerating

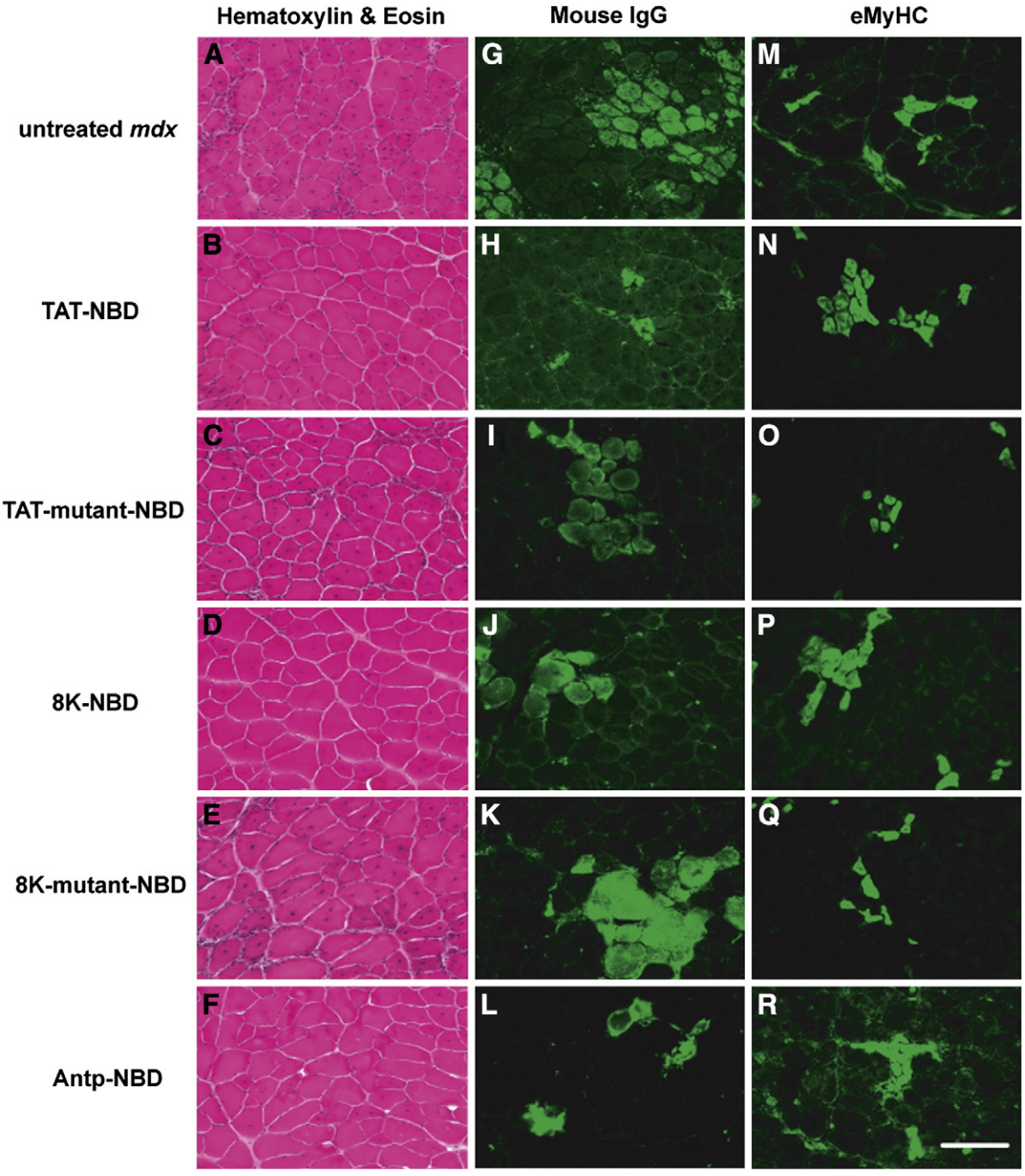

Fig. 2. Histological analysis of *mdx* tibialis anterior muscle histopathology after 4 weeks of PTD-NBD peptide-mediated therapy. 10 μm tibialis anterior muscle sections from age-matched control *mdx* mice, PTD-NBD wild type peptide-treated *mdx* mice, and PTD-NBD mutant peptide treated *mdx* mice were stained with hematoxylin and eosin for gross morphology (A–F), labeled with mouse IgG for detection of necrotic fibers (G–L), and immunostained for embryonic myosin heavy chain for detection of regenerating fibers (M–R). Representative images for each treatment group are shown. Bar represents 100 μm.

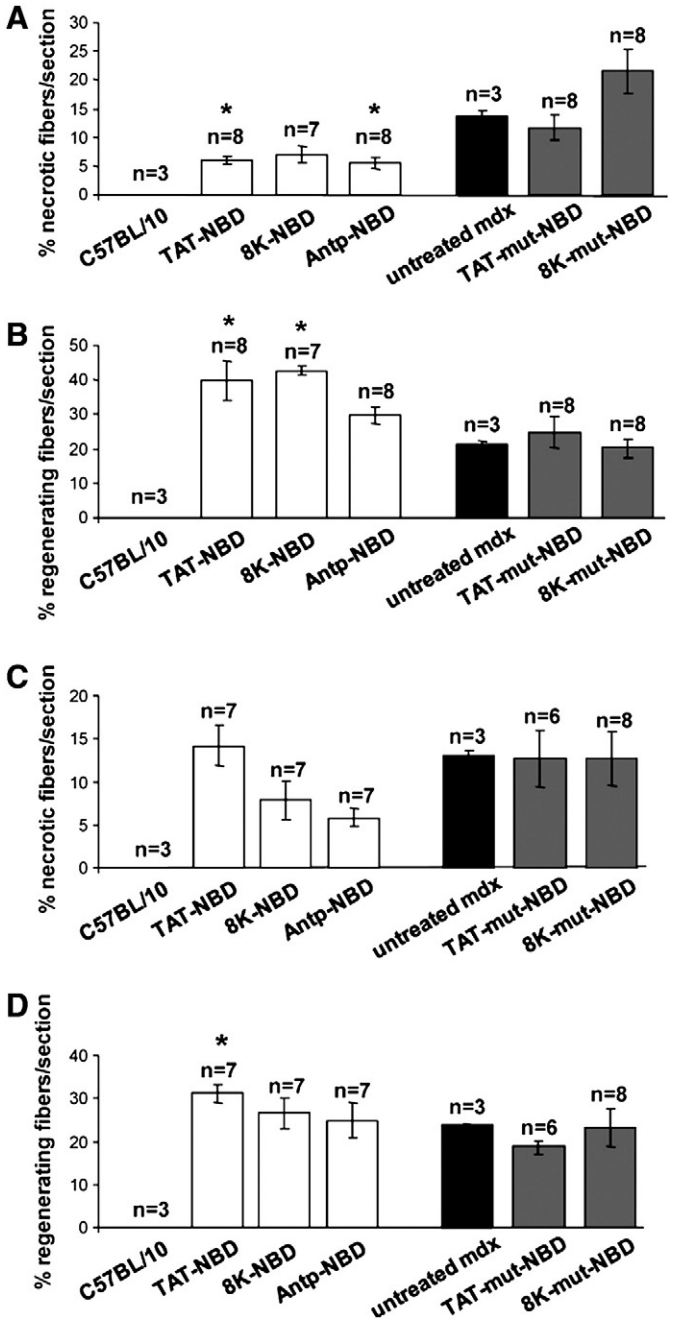

Fig. 3. Quantification of *mdx* tibialis anterior and diaphragm histopathology after 4 weeks of PTD-NBD peptide-mediated therapy. 10 μm muscle sections from age-matched control C57BL/10 and *mdx* mice, PTD-NBD wild type peptide-treated *mdx* and PTD-NBD mutant peptide-treated *mdx* mice were quantified to assess levels of necrosis (A) and regeneration (B) in tibialis anterior muscle and necrosis (C) and regeneration (D) in diaphragm muscle. Data is represented as mean % necrotic or regenerating fibers ± standard error quantified from 2 representative sections per muscle. *Indicates that the PTD-NBD peptide treatment group is significantly different from untreated *mdx* control animals ($p<0.05$). n = number of animals analyzed.

muscle fibers in untreated age-matched *mdx* mice demonstrated an average of 21.3% ± 1.1% regenerating fibers per section. Wild-type PTD-NBD treated groups showed increased numbers of eMyHC-positive fibers compared to *mdx* control animals in the TAT-NBD, 8K-NBD and Antp-NBD fusion peptide treated groups, with increases of 85.6%, 100.3%, and 38.7%, respectively. TAT-NBD and 8K-NBD fusion peptide treated groups showed statistically significant ($p = 0.0494$ and $p = 0.0232$, respectively) increases in the number of regenerating muscle fibers compared to untreated age-matched *mdx* control mice. Similar to the assay of necrosis, mutant peptide treatment did not result in significant changes in the levels of regenerating muscle fibers.

Analysis of diaphragm following 4 weeks of PTD-NBD treatment

Diaphragm tissue from untreated age-matched, wild-type and mutant PTD-NBD peptide treated *mdx* mice were analyzed for levels of necrosis and regeneration after 4 weeks of treatment. Histological analysis with hematoxylin and eosin staining and IgG labeling of necrotic fibers are shown in Fig. 4. Untreated, age-matched control *mdx* mice had an average of 13.0% ± 0.66% necrotic fibers per section (Fig. 3C). In the 4 week wild-type PTD-NBD peptide groups, the number of necrotic fibers in the *mdx* diaphragm decreased by 39.8% and 55.4% in response to the 8K-NBD and Antp-NBD peptide, respectively. TAT-NBD peptide and mutant PTD-NBD peptide treatment did not alter the levels of necrosis in the diaphragm of treated *mdx* mice.

Analysis of eMyHC immunostaining revealed that untreated age-matched *mdx* mice had 23.6% ± 0.52% regenerating fibers per section in the diaphragm (Figs. 3D and 4). Only the wild-type TAT-NBD peptide demonstrated an effect on regeneration, showing a 32.4% increase compared to *mdx* untreated control animals. Mutant PTD-NBD peptide treatment had no significant effect on levels of regeneration in the diaphragm compared to age-matched control *mdx* mice.

Analysis of tibialis anterior muscle after 7 weeks of PTD-NBD treatment

Following 7 weeks of PTD-NBD peptide treatment, we observed improved histopathology in the tibialis anterior muscle of dystrophic *mdx* mice treated with 8K- and TAT-NBD peptides, as compared to saline treated *mdx* controls, which correlated with decreased NF-κB activation in muscle tissue (Figs. 5A and B). Hematoxylin and eosin stained muscle sections revealed less cellular infiltrate and necrosis in PTD-NBD peptide treated *mdx* mice (Figs. 6A–C). Quantitative analysis of saline treated *mdx* control tibialis anterior sections averaged 34 ± 14 necrotic fibers/section, while tissue from 8K- and TAT-NBD peptide treated *mdx* mice average 13 ± 5 and 14 ± 6 necrotic fibers/section, corresponding to decreases in necrotic fibers by 61.8% and 58.8%, respectively (Fig. 7A). 8K- and TAT-NBD peptide treated *mdx* mice demonstrated a 51.2% and 13.5% increase in eMyHC positive, regenerating fibers in the tibialis anterior muscle when compared to saline treated *mdx* controls (Fig. 7B).

Analysis of costal diaphragm after 7 weeks of PTD-NBD treatment

In the costal diaphragm of 7 week PTD-NBD peptide treated *mdx* mice, we observed improved dystrophic histopathology characterized by decreased cellular infiltrate, smaller regions of necrosis, and less fiber size variability, as compared to saline treated *mdx* mice (Figs. 6D–F). The observed improvements in muscle histology in PTD-NBD peptide treated *mdx* mice correlated with decreased levels of NF-κB activation in diaphragm tissue (Figs. 5C and D). Quantitative assessments of necrotic fibers in saline treated *mdx* mice revealed 38 ± 10 necrotic fibers per section. 8K- and TAT-NBD peptide treated *mdx* mice had 27 ± 6 and 18 ± 5 necrotic fibers per section, a decrease of 30.2% and 52.5%, respectively, compared to saline treated *mdx* mice (Fig. 7C). Muscle regeneration observed in the costal diaphragms after 7 weeks of 8K- and TAT-NBD peptide treatment of *mdx* mice revealed increases of 17.5% and 30.1%, respectively, compared to saline treated *mdx* mice (Fig. 7D). TAT-NBD fusion peptide treated *mdx* mice showed statistically significant ($p = 0.0009$) decreases in the number of necrotic muscle fibers compared to saline treated *mdx* control mice. Otherwise, an overall trend toward the decreased number of necrotic fibers and increased number of regenerating fibers in the diaphragm with 8K- and

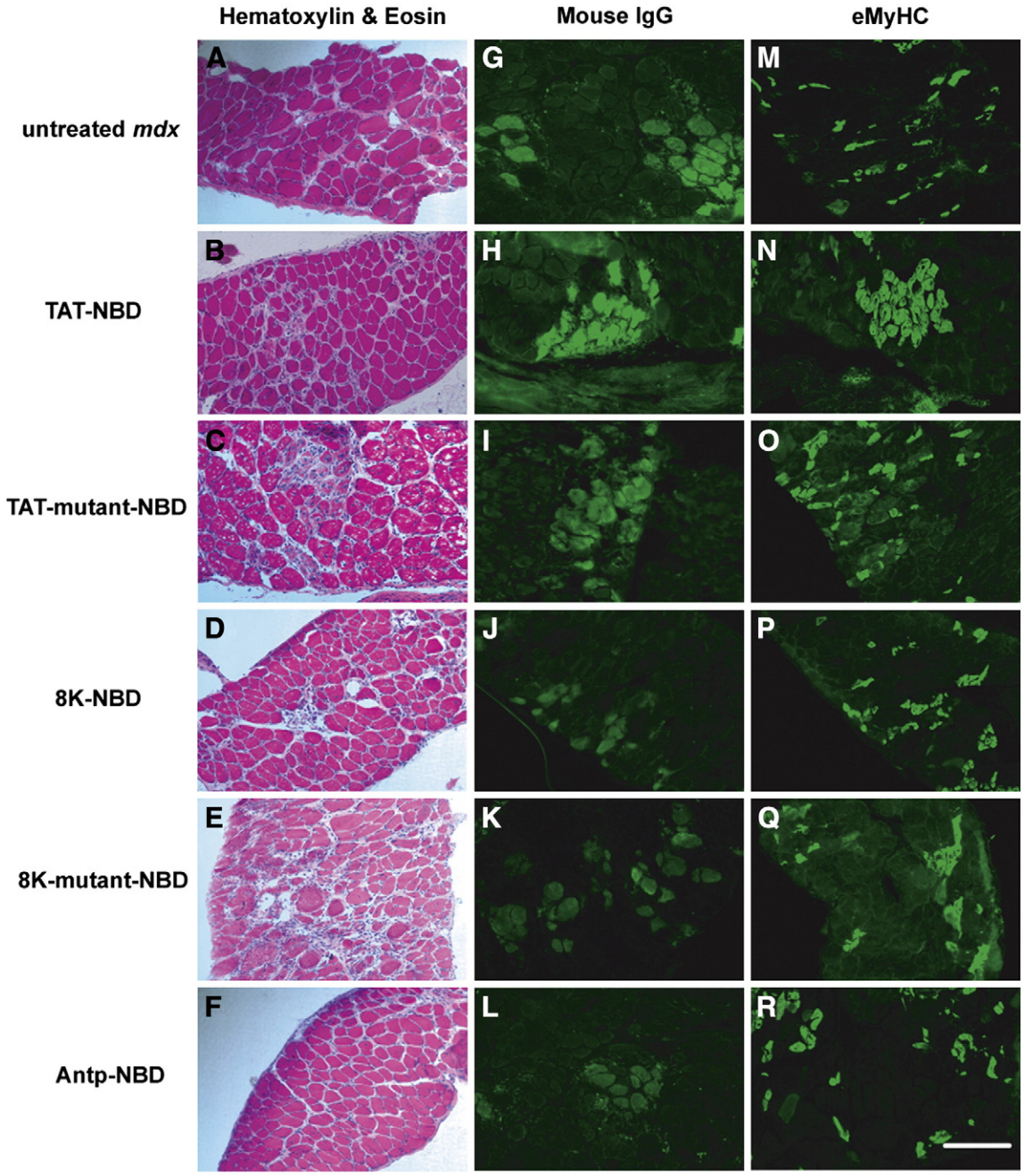

Fig. 4. Histological analysis of *mdx* diaphragm muscle histopathology after 4 weeks of PTD-NBD peptide-mediated therapy. 10 μm sections of diaphragm muscle from age-matched control *mdx* mice, 8K-, TAT-, and Antp-NBD wild type peptide-treated *mdx* mice, and 8K- and TAT-NBD mutant peptide-treated *mdx* mice were stained with hematoxylin and eosin for gross morphology (A–F), labeled with mouse IgG for detection of necrotic fibers (G–L), and immunostained for embryonic myosin heavy chain for detection of regenerating fibers (M–R). Representative images for each treatment group are shown. Bar represents 100 μm.

TAT-NBD fusion peptide treatment compared to saline treated *mdx* control animals was observed. However, these treatment effects were not statistically significant.

Ex vivo costal diaphragm functional assay

The observed improvements in muscle histopathology with PTD-NBD peptide treatment prompted us to explore the effect of PTD-NBD peptide treatment on the physiological function of the diaphragm compared to age-matched, saline treated *mdx* and C57BL/10 controls. Diaphragm from age-matched C57BL/10 normal mice demonstrated the highest average specific force of 30.2 ± 5 N/cm^2, which was significantly higher than all other groups ($p \leq 0.0001$) (Fig. 8A). Diaphragms from saline treated *mdx* mice showed an average specific force of 13 ± 2 N/cm^2, representing a 57.1% decrease from C57BL/10 mice. Diaphragm from *mdx* mice treated with 7 weeks of 8K-NBD or TAT-NBD peptide treated *mdx* mice had an average specific force of 16.6 ± 5 N/cm^2 and 17.1 ± 2 N/cm^2, respectively, representing a 28.2% and 32.1% increase, respectively, over saline treated *mdx* controls. The specific force of the costal diaphragm of 8K- and TAT-NBD peptide treated *mdx* mice were both significantly higher than saline *mdx* controls ($p = 0.0086$ and $p = 0.0234$, respectively).

The response of muscle to repetitive lengthening activations reflects the muscle's ability to sustain force in a paradigm of physiological stress. Relative changes (% baseline) in force during the isometric phase of ten repetitive isovelocity lengthening activations in

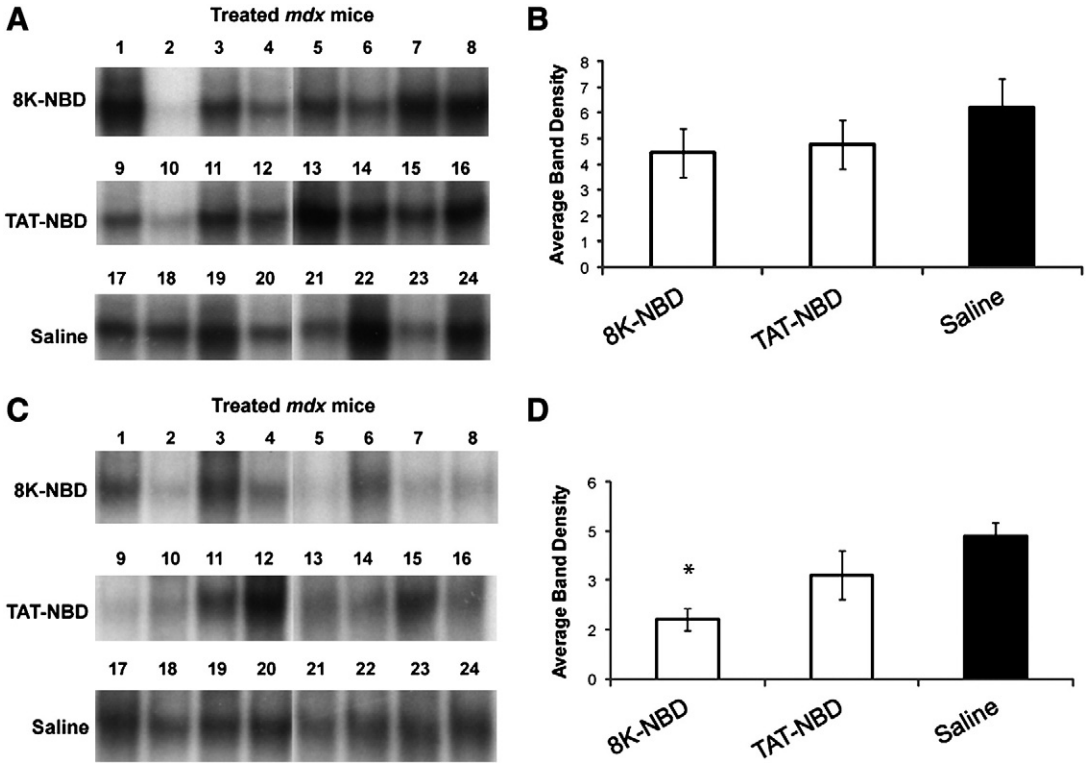

Fig. 5. EMSA analysis of NF-κB activation after 7 weeks of PTD-NBD peptide or saline treatment of *mdx* mice. Nuclear extracts of muscle tissue collected from *mdx* mice after treatment for 7 weeks with 8K- or TAT-NBD peptide, or saline were analyzed for NF-κB activation in the tibialis anterior (A and B) and costal diaphragm (C and D) muscles by electrophoretic mobility shift assay (EMSA). Individual lanes in A and C each show the level of NF-κB in nuclear extract from one animal in the study ($n = 8$ mice/group). Mouse numbers indicate corresponding tibialis anterior and diaphragm samples taken from the same mouse. Panels B and D show densitometric analysis of blots shown in A and C, respectively, represented as mean ± standard error. *Indicates that the PTD-NBD peptide treatment group is significantly different from saline *mdx* control animals ($p < 0.05$).

which the diaphragm was stretched to 110% of resting length were determined (Watchko et al., 2002, 1994). The lowest decrement of force with repetitive lengthening activations was observed in normal C57BL/10 mouse diaphragm (Fig. 8B). The average force generated by the final activation was 94.5% of the initial activation, significantly different from TAT-NBD peptide treated *mdx* mice ($p = 0.0261$) and saline treated *mdx* controls ($p = 0.0002$). Saline treated *mdx* mice exhibited the greatest decrement of force, with the average force generated by the final activation at only 77.2% of the initial activation. The average force generated by the final activation of diaphragm from *mdx* mice after 7 weeks of treatment with 8K- and TAT-NBD peptide was 88.3% and 83.4% of the initial activation, respectively, demonstrating an increased protection from contraction-induced injury as compared to saline treated *mdx* mice. 8K-NBD peptide treated *mdx* mice demonstrated significantly greater force compared with saline treated *mdx* mice ($p = 0.0086$) and was not significantly different from C57BL/10 mice ($p = 0.2212$).

Discussion and conclusions

The decline in function of dystrophin-deficient skeletal muscle is due to progressive muscle necrosis and the ultimate failure of muscle regeneration. Prior studies demonstrated that NF-κB signaling is central to the processes of inflammation, necrosis and regeneration in dystrophin-deficient muscle (Acharyya et al., 2007). Therefore, we expanded on a prior study demonstrating the potential of the Antp-NBD peptide to ameliorate the pathology of dystrophin-deficient limb muscle (Acharyya et al., 2007). In this study we demonstrated that systemic delivery of the NBD peptide fused to multiple different PTDs was effective in decreasing necrosis and increasing regeneration of dystrophin-deficient muscle. The therapeutic effect was observed in diaphragm muscle and was confirmed in limb muscle of the *mdx* mouse model of DMD. The observed effect on diaphragm muscle histology and our demonstration of improved *ex vivo* physiological function, as measured by specific force and response to repetitive lengthening activations, is significant because of the more severe histological phenotype in the *mdx* mouse diaphragm, which provides the best histological model of the changes observed in human DMD muscle (Stedman et al., 1991).

The rationale for delivering PTD-NBD peptides for the treatment of DMD is based on increased levels of activated NF-κB and cytokine production in dystrophic muscle (Acharyya et al., 2007; Dogra et al., 2008; Hnia et al., 2007; Kumar and Boriek, 2003; Messina et al., 2004, 2006; Whitehead et al., 2008). Furthermore, heterozygous deletion of the NF-κB p65 subunit on the *mdx* genetic background demonstrated improved muscle pathology compared to age matched *mdx* mice (Acharyya et al., 2007). In this study, we experimentally demonstrated that multiple PTD-NBD peptides interrupt NF-κB activation, presumably by the disruption of the IKK complex. This disruption is predicted to modulate downstream events in the NF-κB signaling pathway, leading to decreased expression of NF-κB dependent pro-inflammatory genes and decreasing NF-κB-mediated repression of genes whose expression is required for muscle regeneration.

Analysis of NF-κB activation by EMSA in normal C57BL/10 and *mdx* mouse muscle confirmed previous studies (Acharyya et al., 2007; Kumar and Boriek, 2003; Messina et al., 2004, 2006). Interestingly, both the diaphragm and hind limb skeletal muscle of 4-week-old C57BL/10 mice revealed increased levels of activated NF-κB, presumably due to the role of NF-κB in key developmental cellular processes. However, by 9 and 12 weeks of age very little NF-κB activation was detected in normal mouse muscle, while the levels of NF-κB activation increased in *mdx* muscle.

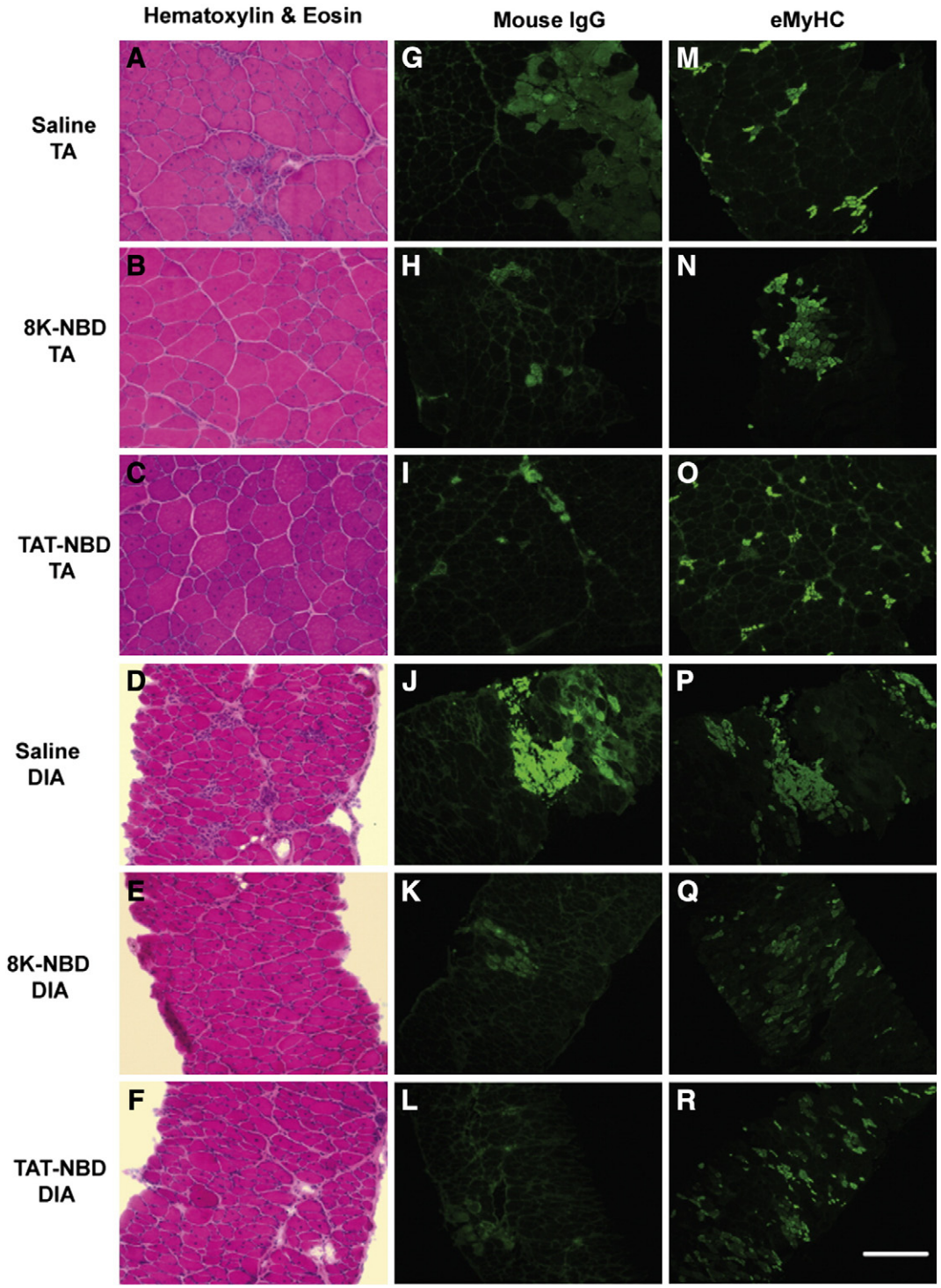

Fig. 6. Histological analysis of *mdx* tibialis anterior and costal diaphragm muscle histopathology after 7 weeks of PTD-NBD peptide-mediated therapy. 10 μm sections of tibialis anterior and costal diaphragm muscle from age-matched saline treated *mdx* mice and 8K- and TAT-NBD peptide-treated *mdx* mice were stained with hematoxylin and eosin for gross morphology (A–F), labeled with mouse IgG for detection of necrotic fibers (G–L), and immunostained for embryonic myosin heavy chain for detection of regenerating fibers (M–R). Representative images for each treatment group are shown. Bar represents 100 μm. TA = tibialis anterior. DIA = diaphragm.

Treatment of *mdx* mice with PTD-NBD peptides, either with a single injection or over a period of 4 or 7 weeks, effectively decreased NF-κB activation in hind limb skeletal muscle and diaphragm, as detected by EMSA, highlighting a critical role that NF-κB plays in dystrophic muscle. From previous studies in other disease models, including neonatal hypoxia–ischemia (Nijboer et al., 2008), collagen induced arthritis (Jimi et al., 2004), and carrageenan-induced paw edema (Di et al., 2005), treatment with PTD-NBD peptide therapy was shown to decrease NF-κB activation, as determined by EMSA, in tissue extracts from brain, ankle joints, and mouse paws, respectively.

In the prior study that demonstrated use of a single PTD-NBD peptide and its effect on hind limb skeletal muscle, 200 μg of Antp-NBD peptide was administered by intraperitoneal injection to 23 day old *mdx* mice every other day for 27 days. Improved muscle histopathology and increased force output was observed in the wild type Antp-NBD peptide treated *mdx* mice compared to those receiving

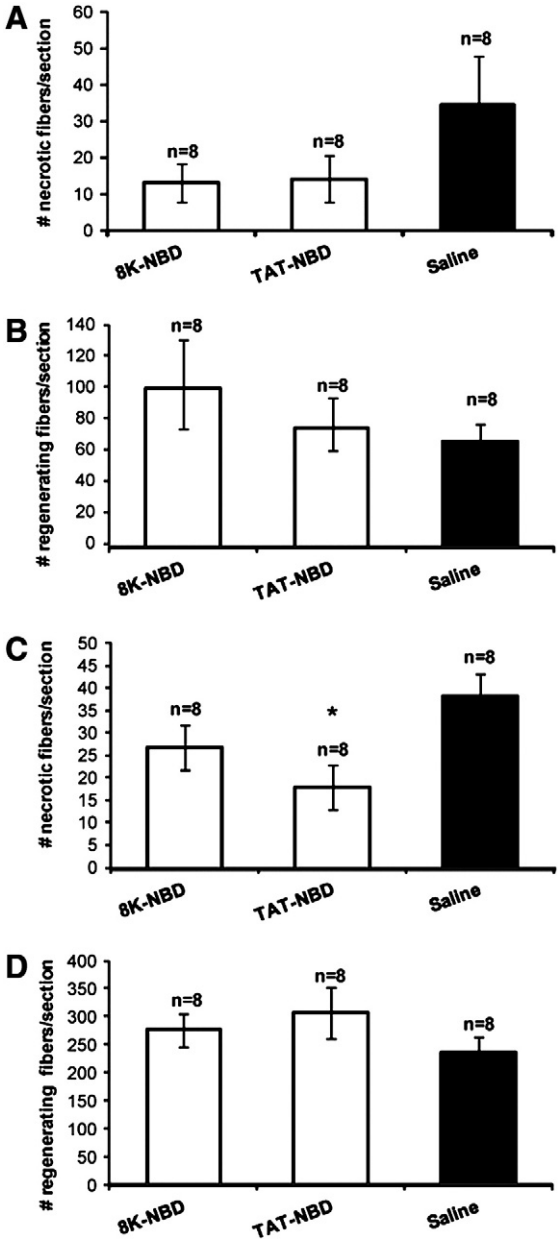

Fig. 7. Quantification of *mdx* tibialis anterior and costal diaphragm muscle histopathology after 7 weeks of PTD-NBD peptide-mediated therapy. 10 μm muscle sections from age-matched, saline treated *mdx* mice, and 8K- and TAT-NBD wild type peptide-treated *mdx* mice were immunostained and quantified to assess levels of necrosis (A) and regeneration (B) in tibialis anterior muscle and necrosis (C) and regeneration (D) in diaphragm muscle. Data is represented as mean total number of necrotic or regenerating fibers ± standard error quantified from 2 representative sections per muscle. *Indicates that the PTD-NBD peptide treatment group is significantly different from saline treated *mdx* control animals ($p<0.05$). n = number of animals analyzed.

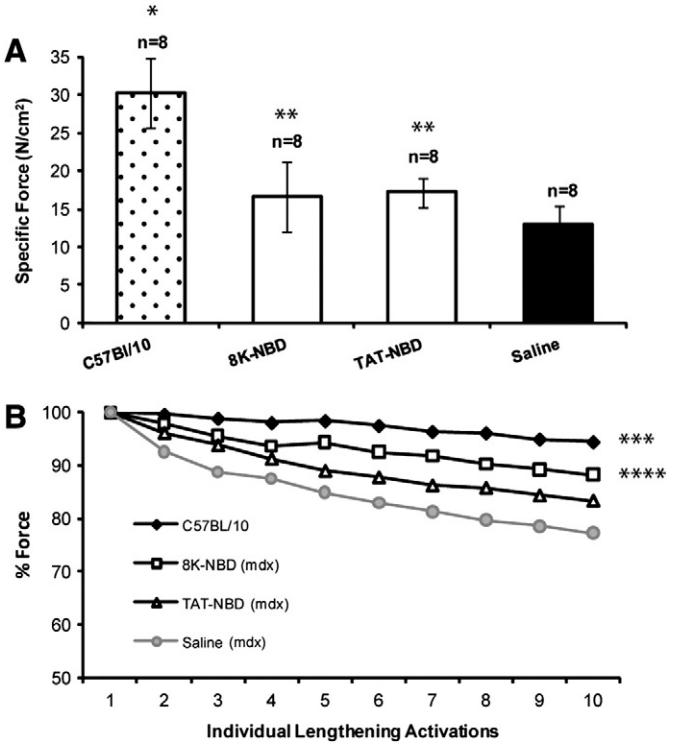

Fig. 8. Force generation properties in *mdx* costal diaphragm after 7 weeks of PTD-NBD peptide therapy. Costal diaphragm muscles were collected after 7 weeks of treatment with 8K- or TAT-NBD peptide or saline. Diaphragms from age-matched control C57BL/10 mice, age-matched saline treated *mdx* mice, and 8K- and TAT-NBD peptide-treated *mdx* mice were analyzed for (A) specific force (N/cm^2) and (B) residual force following 10 repetitive lengthening activations. Lengthening activation data is expressed as a percentage of the force generated in response to the first lengthening activation. The data is shown as mean ± standard error. *Indicates that the C57BL/10 group is significantly different from 8K-NBD, TAT-NBD and saline treated *mdx* mice ($p<0.05$). **Indicates that PTD-NBD peptide treated groups are significantly different from saline treated *mdx* mice ($p<0.05$). ***Indicates that the C57BL/10 group is significantly different from TAT-NBD and saline treated *mdx* mice ($p<0.05$). ****Indicates that the 8K-NBD peptide group is significantly different from saline treated *mdx* mice ($p<0.05$), but not significantly different from C57BL/10 mice. n = number of animals analyzed.

mutant peptide (Acharyya et al., 2007). The present study builds on this prior data to demonstrate that 8K and TAT are also effective PTDs for the systemic delivery of NBD peptide to skeletal muscle. All 3 PTDs were effective and no single PTD stood out as consistently superior to any other when viewed over 2 muscle types (limb and diaphragm) and 2 lengths of treatment (4 and 7 weeks).

Some observed differences across the experiments reported here provide further insights into the treatment of dystrophic muscle with NBD peptide-mediated inhibition of NF-κB activation. In the tibialis anterior muscle of mice treated for 4 weeks, there was improvement in dystrophic histopathology, decreased necrotic fibers and increased levels of muscle fiber regeneration, compared to age-matched untreated *mdx* mice. Following 7 weeks of treatment, we observed continued protection of the tibialis anterior muscle from necrosis with each of the PTD-NBD peptides, but there was a lower effect at this time point. The temporal pattern of degeneration and regeneration in *mdx* skeletal muscle is characterized by an increase in the degree of pathological changes of limb muscle degeneration and regeneration between 4 and 10 weeks of age in *mdx* mice (Grounds et al., 2008). By 12 weeks of age, progressive degeneration and regeneration in *mdx* limb muscle continues at a lower level. Consistent with this, we did not observe an increase in activated NF-κB levels by EMSA in hind limb muscle between 9 and 12 weeks of age.

In contrast in diaphragm muscle, we demonstrated that NF-κB activation levels increase between 9 and 12 weeks of age. In diaphragm, we observed a trend towards improved histopathology after 4 weeks of PTD-NBD peptide delivery and this trend continued following 7 weeks of PTD-NBD peptide treatment. Diaphragm pathology in *mdx* mice more closely models the dystrophic pathology of human DMD muscle with progressive degeneration, attempted regeneration that ultimately fails and replacement with connective tissue (Lynch et al., 1997; Niebroj-Dobosz et al., 1997; Stedman et al., 1991). Since we observed increasing levels of NF-κB activation in diaphragm muscle tissue between 9 and 12 weeks of age, the ongoing benefit seen over time in *mdx* diaphragm with continued treatment by PTD-NBD peptide in our study is encouraging for its ultimate therapeutic utility.

The improvements observed in the functional properties of the costal diaphragm reflected in specific force production and the response to repetitive lengthening activations demonstrates a functional correlate to the improvements observed in histopathology. We demonstrate that mice treated with either the 8K- or TAT-NBD peptide show significantly higher specific force production compared to saline treated *mdx* mice. Additionally, both of the peptide treated *mdx* mice groups had greater sustained force production following repetitive lengthening activations compared to saline treated *mdx* mice after each individual lengthening activation. However, *mdx* mice treated with 8K-NBD peptide achieved the greatest functional correction, as measured by repetitive lengthening activations; 8K-NBD peptide treated *mdx* mice were significantly different from saline treated *mdx* mice, and not significantly different from the C57BL/10 control mice group. Provision of a functional benefit to respiration, which is a vital physiological process, by systemic administration of PTD-NBD peptide to a murine model of dystrophin deficiency suggests a clinically significant treatment effect in this preclinical model of DMD.

Our findings strongly support an *in vivo* mechanism of NBD peptide therapy in muscle. The beneficial effect on necrosis and regeneration in dystrophic muscle reflects the effect of decreased NF-κB activation on downstream targets of the NF-κB pathway. We hypothesize that a lower level of NF-κB activation decreases the inflammatory microenvironment in dystrophic skeletal muscle and this in turn plays a role in the decreased necrosis and increased regeneration observed in PTD-NBD peptide treated *mdx* mouse muscle. Reactive oxygen species (ROS) are increased in pre-necrotic dystrophic muscles (Disatnik et al., 1998), and have been shown to activate the NF-κB pathway (Kumar and Boriek, 2003; Whitehead et al., 2006). A previous study utilizing the anti-oxidant *N*-acetylcysteine in *mdx* mice resulted in significant reduction in ROS in muscle cells in conjunction with increased force output following stretch-induced injury and decreased centralized nuclei in hind limb muscle (Whitehead et al., 2008). The increased levels of ROS in dystrophic muscle coupled with the ability of ROS to activate NF-κB, in addition to knowledge that NF-κB regulates pro-inflammatory cytokines, such as TNF-α and IL-1β, which are also elevated in dystrophic tissue, present a complex picture of activation and feedback loops that contribute to the inflammatory response in muscular dystrophy (Kumar and Boriek, 2003). Future studies will need to comprehensively examine these relationships to determine how PTD-NBD fusion peptide treatment affects this balance.

Administration of PTD-NBD peptides by intraperitoneal injection is a relatively non-invasive means of therapy and offers the advantage of treating a disease of widespread muscle tissue by systemic delivery. However, it is difficult to determine the biodistribution of PTD-NBD peptides in treated mice and whether there are effects on other non-target organs. Evaluation of serum creatine kinase levels from *mdx* mice treated with PTD-NBD peptide for 4 weeks did not show different results from untreated *mdx* controls (data not shown). The demonstration that NF-κB activation is decreased in muscle of treated mice indicates that the NBD peptide is active in muscle tissue following intraperitoneal delivery. Dosage studies will be required to determine the optimal treatment effect and the potential effects on non-target tissues.

In this study, the use of PTD-NBD peptide therapy for treatment of dystrophic muscle of *mdx* mice supports continued research toward its use for DMD patients. While the primary cause of DMD is the lack of a functional dystrophin protein to maintain structural and signaling links from the internal cytoskeleton to the extracellular matrix of muscle cells, therapies that limit inflammation associated with dystrophy and promote muscle regeneration could serve a critical therapeutic purpose. Highly effective treatment of DMD has been elusive to date due to the extent of affected muscle tissue, eventual exhaustion of muscle satellite cells and persistence of inflammation. PTD-NBD peptide therapy has potential both as a primary treatment for DMD and as an adjunct to dystrophin gene transfer.

Acknowledgments

This work was supported by a Department of Defense grant (PRC), a VA Merit Review grant, and Muscular Dystrophy Association grants (PDR), U54 AR50733 (PDR) and U01 NS069562 (DCG, PDR and PRC). The authors take full responsibility for the contents of this paper, which do not represent the views of the Department of Veterans Affairs or the United States Government.

References

Acharyya, S., Villalta, S.A., Bakkar, N., Bupha-Intr, T., Janssen, P.M.L., Carathers, M., et al., 2007. Interplay of IKK/NF-kappa B signaling in macrophages and myofibers promotes muscle degeneration in Duchenne muscular dystrophy. J. Clin. Invest. 117, 889–901.

Bulfield, Siller, W.G., Wight, P.A., Moore, K.J., 1984. X chromosome-linked muscular dystrophy (mdx) in the mouse. Proc. Natl. Acad. Sci. U. S. A. 81, 1189–1192.

Dave, S.H., Tilstra, J.S., Matsuoka, K., Li, F., Karrasch, T., Uno, J.K., et al., 2007. Amelioration of chronic murine colitis by peptide-mediated transduction of the IkappaB kinase inhibitor NEMO binding domain peptide. J. Immunol. 179, 7852–7859.

Di, M.P., Ianaro, A., Ghosh, S., 2005. Amelioration of acute inflammation by systemic administration of a cell-permeable peptide inhibitor of NF-kappaB activation. Arthritis Rheum. 52, 951–958.

Disatnik, M.H., Dhawan, J., Yu, Y., Beal, M.F., Whirl, M.M., Franco, A.A., et al., 1998. Evidence of oxidative stress in mdx mouse muscle: studies of the pre-necrotic state. J. Neurol. Sci. 161, 77–84.

Dogra, C., Srivastava, D.S., Kumar, A., 2008. Protein–DNA array-based identification of transcription factor activities differentially regulated in skeletal muscle of normal and dystrophin-deficient mdx mice. Mol. Cell. Biochem. 312, 17–24.

Ervasti, J., Campbell, K., 1991. Membrane organization of the dystrophin–glycoprotein complex. Cell 66, 1121–1131.

Ervasti, J., Ohlendieck, K., Kahl, S., Gaver, M., Campbell, K., 1990. Deficiency of a glycoprotein component of the dystrophin complex in dystrophic muscle. Nature 345, 315–319.

Grounds, M.D., Torrisi, J., 2004. Anti-TNF alpha (Remicade (R)) therapy protects dystrophic skeletal muscle from necrosis. FASEB J. 18, 676–682.

Grounds, M.D., Radley, H.G., Lynch, G.S., Nagaraju, K., De, L.A., 2008. Towards developing standard operating procedures for pre-clinical testing in the mdx mouse model of Duchenne muscular dystrophy. Neurobiol. Dis. 31, 1–19.

Guttridge, D., 2004. Signaling pathways weigh in on decisions to make or break skeletal muscle. Curr. Opin. Clin. Nutr. Metab. Care 7, 443–450.

Guttridge, D.C., Albanese, C., Reuther, J.Y., Pestell, R.G., Baldwin, A.S., 1999. NF-kappa B controls cell growth and differentiation through transcriptional regulation of cyclin D1. Mol. Cell. Biol. 19, 5785–5799.

Häcker, H., Karin, M., 2006. Regulation and function of IKK and IKK-related kinases. Sci. Signal. 357, 1–19.

Hakansson, S., Jacobs, A., Caffrey, M., 2001. Heparin binding by the HIV-1 tat protein transduction domain. Protein Sci. 10, 2138–2139.

Hnia, K., Hugon, G., Rivier, F., Masmoudi, A., Mercier, J., Mornet, D., 2007. Modulation of p38 mitogen-activated protein kinase cascade and metalloproteinase activity in diaphragm muscle in response to free radical scavenger administration in dystrophin-deficient mdx mice. Am. J. Pathol. 170, 633–643.

Jimi, E., Aoki, K., Saito, H., D'Acquisto, F., May, M.J., Nakamura, I., et al., 2004. Selective inhibition of NF-kappa B blocks osteoclastogenesis and prevents inflammatory bone destruction in vivo. Nat. Med. 10, 617–624.

Khaja, K., Robbins, P., 2010. Comparison of functional protein transduction domains using the NEMO binding domain peptide. Pharmaceuticals 3, 110–124.

Kumar, A., Boriek, A.M., 2003. Mechanical stress activates the nuclear factor-kappaB pathway in skeletal muscle fibers: a possible role in Duchenne muscular dystrophy. FASEB J. 17, 386–396.

Lynch, G.S., Rafael, J.A., Hinkle, R.T., Cole, N.M., Chamberlain, J.S., Faulkner, J.A., 1997. Contractile properties of diaphragm muscle segments from old mdx and old transgenic mdx mice. Am. J. Physiol. 272, C2063–C2068.

May, M.J., D'Acquisto, F., Madge, L.A., Glockner, J., Pober, J.S., Ghosh, S., 2000. Selective inhibition of NF-kappaB activation by a peptide that blocks the interaction of NEMO with the IkappaB kinase complex. Science 289, 1550–1554.

Messina, S., Seminara, P., Aguennouz, M., Monici, M.C., Marini, H., Squadrito, F., et al., 2004. NF-kB blockade reduces skeletal muscle degeneration and enhances muscle function in mdx mice. Neuromuscul. Disord. 14, 234–241.

Messina, S., Altavilla, D., Aguennouz, M., Seminara, P., Minutoli, L., Monici, M.C., et al., 2006. Lipid peroxidation inhibition blunts nuclear factor-kappaB activation, reduces skeletal muscle degeneration, and enhances muscle function in mdx mice. Am. J. Pathol. 168, 918–926.

Mi, Z., Mai, J., Lu, X., Robbins, P.D., 2000. Characterization of a class of cationic peptides able to facilitate efficient protein transduction in vitro and in vivo. Mol. Ther. 2, 339–347.

Niebroj-Dobosz, I., Fidzianska, A., Glinka, Z., 1997. Comparative studies of hind limb and diaphragm muscles of mdx mice. Basic Appl Myol. 7, 381–386.

Nijboer, C.H., Heijnen, C.J., Groenendaal, F., May, M.J., van Bell, F., Kavelaars, A., 2008. Strong neuroprotection by inhibition of NF-kappaB after neonatal hypoxia–ischemia involves apoptotic mechanisms but is independent of cytokines. Stroke 39, 2129–2137.

Noguchi, H., Matsumoto, S., 2006. Protein transduction technology: a novel therapeutic perspective. Acta Med. Okayama 60, 1–11.
Rusnati, M., Coltrini, D., Oreste, P., Zoppetti, G., Albini, A., Noonan, D., et al., 1997. Interaction of HIV-1 Tat protein with heparin. Role of the backbone structure, sulfation, and size. J. Biol. Chem. 272, 11313–11320.
Schwarze, S.R., Ho, A., Vocero-Akbani, A., Dowdy, S.F., 1999. In vivo protein transduction: delivery of a biologically active protein into the mouse. Science 285, 1569–1572.
Stedman, H.H., Sweeney, H.L., Shrager, J.B., Maguire, H.C., Panettieri, R.A., Petrof, B., et al., 1991. The mdx mouse diaphragm reproduces the degenerative changes of Duchenne muscular dystrophy. Nature 352, 536–539.
Strickland, I., Ghosh, S., 2006. Use of cell permeable NBD peptides for suppression of inflammation. Ann. Rheum. Dis. 65, 75–82.
Tilstra, J., Rehman, K.K., Hennon, T., Plevy, S.E., Clemens, P., Robbins, P.D., 2007. Protein transduction: identification, characterization and optimization. Biochem. Soc. Trans. 35, 811–815.
Verma, I., 2004. Nuclear factor (NF)-kappa B proteins: therapeutic targets. Ann. Rheum. Dis. 63, 57–61.
Watchko, J.F., Johnson, B.D., Gosselin, L.E., Prakash, Y.S., Sieck, G.C., 1994. Age-related differences in diaphragm muscle injury after lengthening activations. J. Appl. Physiol. 77, 2125–2133.
Watchko, J., O'Day, T., Wang, B., Zhou, L., Tang, Y., Li, J., et al., 2002. Adeno-associated virus vector-mediated minidystrophin gene therapy improves dystrophic muscle contractile function in mdx mice. Hum. Gene Ther. 13, 1451–1460.
Whitehead, N.P., Yeung, E.W., Allen, D.G., 2006. Muscle damage in mdx (dystrophic) mice: role of calcium and reactive oxygen species. Clin. Exp. Pharmacol. Physiol. 33, 657–662.
Whitehead, N.P., Pham, C., Gervasio, O.L., Allen, D.G., 2008. N-Acetylcysteine ameliorates skeletal muscle pathophysiology in mdx mice. J. Physiol. 586, 2003–2014.
Zubrzycka-Gaarn, E.E., Bulman, D.E., Karpati, G., Burghes, A.H., Belfall, B., Klamut, H.J., et al., 1988. The Duchenne muscular dystrophy gene product is localized in sarcolemma of human skeletal muscle. Nature 333, 466–469.